NUMERICAL OPTIMAL CONTROL OF INSTATIONARY GAS TRANSPORT WITH CONTROL AND STATE CONSTRAINTS

H. EGGER AND T. KUGLER AND W. WOLLNER

Department of Mathematics, TU Darmstadt, Germany

Abstract. We consider the optimal control of a nonlinear hyperbolic system of balance laws on a one-dimensional network which arises in the context of gas transport in pipeline systems. State constraints, which are required for the safe operation of the system, are incorporated by a barrier method. We discuss the well-posedness of the governing system of partial differential-algebraic equations and investigate the existence of minimizers. For the numerical solution, we then consider the approximation of the state equation by mixed finite elements in space and a particular linear implicit time integration scheme that can be interpreted as a discontinuous Galerkin approximation. We establish well-posedness of this discretization scheme and prove the existence of minimizers for the corresponding discretized optimal control problem and discuss its numerical solution by a projected Gauß-Newton method. The efficient realization of the Jacobian and Hessian of the quadratic approximations that have to be minimized in every iteration of the Gauß-Newton method can be obtained via the solution of discretized sensitivity and adjoint equations. These are obtained by formal differentiation and transposition of the Galerkin methods employed for the discretization of the state equations. All approximations obtained after discretization can thus be interpreted as functions on the continuous level and, since the functional analytic setting is not changed by the Galerkin discretization, we observe mesh independence of the resulting fully discrete methods. For illustration of our theoretical results and to demonstrate the efficiency of the proposed method, we present numerical results for two test problems that model typical situations that may arise in the daily operation of gas networks.

Keywords:

AMS-classification (2000):

1. Introduction

We study the optimal control of a transport network and its efficient numerical realization. Such problems arise in various applications, e.g., in traffic flow control [13], in supply chains [11, 19], in water supply systems [7], or in gas transport [29]. This paper is motivated by and addresses the latter. Due to its practical relevance, there has been intensive research on the optimization and optimal control of gas networks. Most of the literature is concerned with strategic planning and stationary flow conditions, in which the gas transport in pipelines can be described by nonlinear algebraic equations. Let us refer to [20, 24] for an overview about stationary gas network optimization and further references.

E-mail address: egger@mathematik.tu-darmstadt.de, kugler@mathematik.tu-darmstadt.de, wollner@mathematik.tu-darmstadt.de.

The instationary gas transport resulting from intraday variations of customer supplies and demands is usually modeled by a system of partial differential-algebraic equations [26, 5] and the corresponding control and optimization problems thus have to be considered formally in an infinite dimensional setting. To overcome the technical difficulties, most of the research starts from a specific discretization of the gas flow equations and then focus on the algorithmic treatment of the optimization problem. Let us briefly mention some of the available results. One of the first references in this context are due Wong and Larson [35, 36], who study dynamic programming approaches for the optimization of natural-gas pipeline systems. They use parabolic models to describe the gas flow. In [32], Stoner considers nonlinear hyperbolic transient and stationary gas flow model and investigates the control of gas transients in single pipelines and on networks. Bamberger, Sorine and Yvone consider in [1] a doubly nonlinear parabolic gas flow model which describes the evolution of the pressure. They prove well-posedness of the state equation and investigate the control of a small network. Furey [10] also uses a parabolic model for gas transport and investigates the use of an SQP strategy for the numerical treatment of the resulting optimal control problem. Mixed integer nonlinear control problems resulting from a discretization of hyperbolic gas flow equations are investigated in [6, 16]. The complexity of the resulting minimization problems allows only for very coarse discretizations of the gas transport through pipelines whose validity in the highly dynamic regime may not be guaranteed. The optimal control of gas transport described by gas flow models of different accuracy is partly investigated in [7]. A simulated annealing approach is considered in [23]. As examples for more theoretical work, let us mention [12, 14], where questions concerning the controllability and feedback stabilization of gas networks are addressed.

In this paper, we study the gas network optimization from the perspective of the optimal control of partial differential equations [22, 33]. In this spirit, we investigate the underlying infinite dimensional problem and derive corresponding numerical approximations in a functional analytic setting. This allows to systematically construct and analyze finite dimensional optimal control problems that result from discretization of the governing system of differential equations. This systematic approach towards the analysis and numerical solution of optimal control problems with partial differential equations is well developed, in particular for problems governed by elliptic and parabolic equations [22, 33]. Let us mention [17, 34] for some recent examples concerning the control of hyperbolic systems.

As a model for the gas transport in pipelines, we utilize a semilinear hyperbolic system which describes the gas flow under isothermal conditions with sufficient accuracy; see [26, 5] for a derivation. Algebraic coupling conditions are used to model the conservation of mass and the balance of energy across pipe junctions and through active elements like compressors or regulators which may be controlled by the user. This results in an optimal control problem governed by a system of partial differential-algebraic equations. In addition, control and state constraints have to be satisfied in order to guarantee the safe operation of the system; the latter may be incorporated by a barrier method [21, 30, 31]. The dynamic request of the customers finally enter via the boundary conditions.

Let us briefly outline the structure and the main contributions of this paper: In Section 2, we introduce in detail the gas transport model and the optimal control problem under investigation in which the state constraints are taken into account by a barrier method. We briefly discuss the well-posedness of the state equations and investigate the

feasibility of the optimization problem. These considerations reveal the appropriate functional analytic setting which is used for the rest of the paper. In Section 3, we present a variational characterization of the solutions to the gas transport model, which allows to construct systematic discretizations by means of Galerkin approximation. We utilize an approximation by mixed finite elements in space and a particular linear implicit time integration scheme which can be interpreted as a discontinuous Galerkin approximation. The discretization of the gas transport model can therefore be considered in the functional analytic setting of the underlying infinite dimensional problem. This allows us to prove the existence and continuous dependence of solutions to the discretized optimal control problem. Due to the variational structure of the discretization schemes, we also avoid some of the problems coming from a first-discretize-then-optimize approach [15, 28]. In Section 4, we discuss the efficient numerical minimization of the discretized optimal control problem by aprojected Gauß-Newton method. We discuss in detail the solution of the corresponding quadratic control problems, arising in every step of the Newton iteration, by means of a conjugate gradient method which only requires the assembly of the Jacobian and the repeated application of the Hessian of the quadratic approximation. The efficient realization of these operations by solution of sensitivity and adjoint equations is discussed. In Section 5, we then illustrate the performance of the proposed algorithms with a few test problems which model typical situations that might occur during intraday operation of a gas network. These tests demonstrate the viability and robustness of the proposed methods and their feasibility for online control. We also demonstrate the mesh independence of the algorithms and of the optimal controls which can be expected, since we respect the underlying functional analytic setting in the discretization process. The presentation closes with a short discussion of our results.

2. Problem formulation

In the following, we introduce in detail the optimal control problem to be considered in the rest of the manuscript. To be as specific as possible, we present our notation and arguments for a particular model problem which will also be addressed in our numerical tests.

2.1. **Geometry.** The topology of the network is modeled by a finite directed and connected graph $(\mathcal{V}, \mathcal{E})$; see Figure 2.1 for an example. To any vertex $v \in \mathcal{V}$ we associate the set $\mathcal{E}(v) = \{e \in \mathcal{E} : e = (v, \cdot) \text{ or } e = (\cdot, v)\}$ of edges which have v as start or endpoint. Any edge $e \in \mathcal{E}$ has the form $e = (v_{in}, v_{out})$ and we define $n_e(v_{in}) = -1$, $n_e(v_{out}) = 1$, and $n_e(v) = 0$ for $v \notin \{v_{in}, v_{out}\}$. The matrix $N \in \{-1, 0, 1\}^{|\mathcal{V}|\times|\mathcal{E}|}$ with entries $N_{i,j} = n_{e_j}(v_i)$ then is the incidence matrix of the graph [2]. The vertex set $\mathcal{V}$ is split by $\mathcal{V} = \mathcal{V}_p \cup \mathcal{V}_m \cup \mathcal{V}_a \cup \mathcal{V}_0$ into boundary vertices with pressure and mass flow conditions, vertices representing active elements, and interior vertices modeling the junction of pipes.

To any edge $e = (v_{in}, v_{out})$, we associate an interval $[0, \ell_e]$ of length $\ell_e > 0$ and we denote by $\ell \in \mathbb{R}^{|\mathcal{E}|}$ the vector with entries ℓ_e. Following the notation of [25], we call $\mathcal{G} = (\mathcal{V}, \mathcal{E}, \ell)$ a geometric graph. In the sequel, we tacitly identify the topological edge e with the interval $[0, \ell_e]$ and we denote by $L^2(\mathcal{E}) = \{f : f|_e = f_e \in L^2(e) = L^2(0, \ell_e)\}$ the

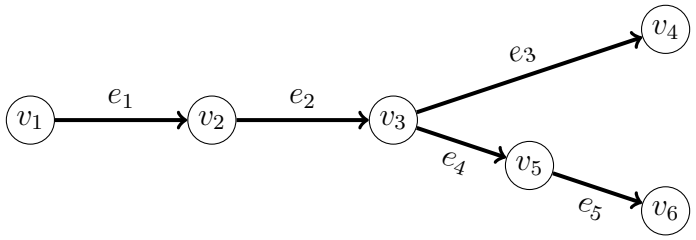

FIGURE 2.1. Directed graph $(\mathcal{V}, \mathcal{E})$ with vertices $\mathcal{V} = \{v_1, \dots, v_6\}$ and edges $\mathcal{E} = \{e_1, \dots, e_5\}$. The incidence coefficients are given by $n_{e_1}(v_1) = n_{e_2}(v_2) = n_{e_3}(v_3) = n_{e_4}(v_3) = n_{e_5}(v_5) = -1$ and $n_{e_1}(v_2) = n_{e_2}(v_3) = n_{e_3}(v_4) = n_{e_4}(v_5) = n_{e_5}(v_6) = 1$. We denote by $\mathcal{V}_p = \{v_1\}$ and $\mathcal{V}_m = \{v_4, v_6\}$ the boundary vertices with pressure and flux boundary conditions, by $\mathcal{V}_0 = \{v_3\}$ the interior junction, and by $\mathcal{V}_a = \{v_2, v_5\}$ the vertices representing active elements like compressors or regulators, respectively.

space of square integrable functions defined on the graph with scalar product

$$(f, g)_{\mathcal{E}} = \sum_{e \in \mathcal{E}} (f, g)_e = \int_0^{\ell_e} f(x) g(x) dx.$$

Further function spaces will be defined below as required.

2.2. **State equations.** Any edge $e \in \mathcal{E}$ of the geometric graph represents a pipe of the network. As a model for the gas flow in the pipes, we use the semilinear hyperbolic system

$$a_e \partial_t p_e + \partial_x m_e = 0 \qquad e \in \mathcal{E}, \tag{2.1}$$

$$b_e \partial_t m_e + \partial_x p_e = -d_e(p_e, m_e) m_e \qquad e \in \mathcal{E}. \tag{2.2}$$

Here p_e and m_e denote, respectively, the pressure and mass flux within the pipe e, and the parameters are defined by $a_e = A_e/c^2$, $b_e = 1/A_e$, where A_e, D_e denote the cross-section and diameter of the pipe, and c is the speed of sound. The damping through friction at the pipe walls is described by the nonlinear function

$$d_e(p_e, m_e) = \max\{\epsilon, \min\{1/\epsilon, \frac{\lambda_e}{2D_e} \frac{c^2}{A_e^2} \frac{|m_e|}{p_e}\}\},$$

where λ_e is the friction factor and $\epsilon \geq 0$ is a truncation parameter. For $\epsilon = 0$, the system (2.1)–(2.2) corresponds to a standard models for gas transport in pipelines, see [4] for a detailed derivation. To avoid technical difficulties, we set $\epsilon > 0$ in the sequel, which does not introduce any perturbation, as long as the pressure and mass flux are suitably bounded. LEt us note that this will be enforced automatically by state constraints in the final optimal control problem. The truncation by $\epsilon > 0$ therefore only serves to simplify the theoretical considerations.

The differential equations on the individual pipes are supplemented by the following coupling and boundary conditions. At internal vertices $v \in \mathcal{V}_0$, we require that

$$\sum_{e \in \mathcal{E}(v)} m_e(v) n_e(v) = 0 \qquad v \in \mathcal{V}_0, \tag{2.3}$$

$$p_e(v) = p_{e'(v)} \qquad e \in \mathcal{E}(v),\ v \in \mathcal{V}_0. \tag{2.4}$$

The vertices $v \in \mathcal{V}_a$ respresent active elements like compressors or regulators and they are assumed to be the intersections of exactly two edges $v = e_{in} \cap e_{out}$. This allows to associate a particular orientation to these vertices which enables us to treat compressors and regulators in a unified manner. For the active vertices, we then require that

$$\sum_{e \in \mathcal{E}(v)} m_e(v) n_e(v) = 0 \qquad v \in \mathcal{V}_a, \tag{2.5}$$

$$p_{e_{out}}(v) = p_{e_{in}}(v) + u_v \qquad v \in \mathcal{V}_a. \tag{2.6}$$

We assume in the sequel that the orientation has been chosen such that $u_v \geq 0$, i.e., the pressure drop across an active element is always positive. A compressor then increases the pressure in flow direction, while a regulator increases the pressure in opposite flow direction, i.e., it effectively decreases pressure. At the boundary vertices $v \in \mathcal{V}_p \cap \mathcal{V}_m$, we require that either the pressure or the mass flux are prescribed by one of the following conditions

$$m_e(v) n_e(v) = \widehat{m}_v \qquad e \in \mathcal{E}(v),\ v \in \mathcal{V}_m, \tag{2.7}$$

$$p_e(v) = \widehat{p}_v \qquad e \in \mathcal{E}(v),\ v \in \mathcal{V}_p. \tag{2.8}$$

All of the above equations (2.1)–(2.8) are tacitly assumed to hold for $t \in [0, T]$, where $T > 0$ is the time horizon of interest. Together with appropriate initial conditions

$$p(0) = \widehat{p}_0, \qquad m(0) = \widehat{m}_0 \qquad \text{on } \mathcal{E}, \tag{2.9}$$

this system of differential and algebraic equations describes the gas flow in the network. The functions $\widehat{p}_v$, $\widehat{m}_v$, $\widehat{p}_0$, $\widehat{m}_0$ and the control functions u_v denote input data.

2.3. **Optimal control problem.** A standard objective in the control of gas networks is to satisfy all consumer demands and at the same time to minimize the fuel consumption of the compressors. For ease of presentation, we assume in the following that $|\mathcal{V}_a| = 1$, i.e., only one active element is present, and we intend to minimize the cost functional

$$\|u\|_{L^1(0,T)} + \frac{\alpha}{2} \|u\|^2_{H^1(0,T)}, \tag{2.10}$$

where $u = u_v$, $v \in \mathcal{V}_a$ is the control arising in (2.6) and $\alpha > 0$ is some regularization parameter. The first term models the cost of operating the active elements and the second term promotes a smooth control behavior. In order to guarantee that the active elements work reliably as desired, we require that

$$0 \leq u_v \leq u_{max,v} \qquad v \in \mathcal{V}_a. \tag{2.11}$$

For the safe operation of the gas network at all times, one has to avoid that the pipes run dry or burst. We therefore assume that gas transport takes place in certain physical ranges and require that

$$0 < p_{min,e} \leq p_e \leq p_{max,e} \qquad e \in \mathcal{E}, \tag{2.12}$$

for appropriate constant lower and upper bounds for the pressure which can be understood as piecewise constant functions p_{min}, p_{max}. These state constraints can be incorporated into the optimization problem by a barrier method. Let us define

$$F(p) = \left(\frac{p_{max}}{p_{max} - p} \right) \left(\frac{p_{max}}{p - p_{min}} \right), \qquad p_{min} < p < p_{max}, \tag{2.13}$$

which is extended by $F(p) = \infty$ for $p \le p_{min}$ and $p \ge p_{max}$. We will use $\|F(p)\|^2_{L^2(0,T;L^2(\mathcal{E}))}$ as a barrier term for the state constraints in the optimization problem which exhibits a quadratic singularity at the boundary of the feasible region.

Remark 2.1. For ease of notation, we assume here and in the following that only one active element is working, i.e., $|\mathcal{V}_a| = 1$. In addition, we only made use of state constraints for the pressure. Corresponding bounds for the mass flux m and multiple active elements can however be taken into account without difficulties; see Section 5 for an example.

In the following sections, we will consider the following control problem.

Problem 2.2 (Optimal control problem)**.**
Given appropriate initial and boundary values $\widehat{p}_0$, $\widehat{m}_0$ and $\widehat{p}_v$, $\widehat{m}_v$, solve

$$\min_{(u,p)} J(u,p) = \|u\|_{L^1(0,T)} + \frac{\alpha}{2}\|u\|^2_{H^1(0,T)} + \frac{\beta}{2}\|F(p)\|^2_{L^2(0,T;L^2(\mathcal{E}))} \tag{2.14}$$
$$\text{subject to (2.1)–(2.9) and (2.11).}$$

Here $L^2(0,T;X)$ denotes the space of functions $f : [0,T] \to X$ with the canonical norm defined by $\|f\|^2_{L^2(0,T;X)} = \int_0^T \|f(t)\|^2_X$. We will show below that for any admissible control

$$u \in U_{ad} = \{u \in H^1(0,T) : \text{s.t. (2.11) holds}\}, \tag{2.15}$$

the states $p = p(u)$, $m = m(u)$ are uniquely determined by the system (2.1)–(2.9) of partial differential-algebraic equations. The states (p,m) can thus be formally eliminated from the system and Problem 2.2 can be written equivalently as follows.

Problem 2.3 (Reduced control problem)**.**
Given appropriate initial and boundary values $\widehat{p}_0$, $\widehat{m}_0$ and $\widehat{p}_v$, $\widehat{m}_v$, solve

$$\min_{u\in U_{ad}} J_R(u) = \|u\|_{L^1(0,T)} + \frac{\alpha}{2}\|u\|^2_{H^1(0,T)} + \frac{\beta}{2}\|F(p(u))\|^2_{L^2(0,T;L^2(\mathcal{E}))} \tag{2.16}$$

where $p(u)$ denotes the pressure component of the solutions of the system (2.1)–(2.9).

Note that the reduced objective functional is simply given by $J_R(u) = J(u,p(u))$ and that the two optimal control problems are equivalent if the pressure $p(u)$ is uniquely defined by the system (2.1)–(2.9). The efficient numerical approximation of the reduced optimal control problem will be the main purpose of the rest of the manuscript.

2.4. **Comments on well-posedness.** Before we turn to the numerical solution of the optimal control problems stated above, let us briefly discuss some analytical aspects of the problems under investigation and illustrate their viability.

Remark 2.4 (Well-posedness of the state system)**.** Problem (2.1)–(2.9) is an initial boundary value problem for a semilinear hyperbolic system. Due to the truncation of the damping term with $\epsilon > 0$, the right hand side in (2.2) is globally Lipschitz continuous, i.e.,

$$\|d_e(p_e,m_e)m_e - d_e(\widetilde{p}_e,\widetilde{m}_e)\widetilde{m}_e\|_{L^2(e)} \le C(\|p_e - \widetilde{p}_e\|_{L^2(e)} + \|m_e - \widetilde{m}_e\|_{L^2(e)})$$

for all $e \in \mathcal{E}$ with uniform constant $C = \frac{3}{\epsilon} + \frac{1}{\epsilon^2}$. After some minor computations, one can therefore deduce from [27, Theorem 6.1.2], that the system (2.1)–(2.9) has a unique mild solution $(p,m) \in C([0,T];L^2(\mathcal{E}) \times L^2(\mathcal{E}))$ whenever the data $\widehat{p}_v$, $\widehat{m}_v$, $\widehat{p}_0$, $\widehat{u}_0$ and the

control function u_v are sufficiently smooth in time. Using standard energy arguments, one can further show that the solution is strong, i.e.,

$$(p, m) \in W^{1,\infty}([0,T]; L^2(\mathcal{E}) \times L^2(\mathcal{E})) \cap L^\infty([0,T]; H^1(\mathcal{E} \setminus \mathcal{V}_a) \cap H(\mathrm{div}; \mathcal{E})),$$

provided that the initial and boundary data and the control are sufficiently smooth and satisfy the usual compatibility conditions; see, e.g., [9] for details. Let us note at this point that $H^1(\mathcal{E} \setminus \mathcal{V}_a) = \{f \in L^2(\mathcal{E}) : f_e \in H^1(e)\ \forall e \in \mathcal{E}$ and (2.4) holds$\}$ consists of pressure functions that may be discontinuous only in the vertices $v \in \mathcal{V}_a$. On the other hand, the space $H(\mathrm{div}; \mathcal{E}) = \{f \in L^2(\mathcal{E}) : f_e \in H^1(\mathcal{E})\ \forall e \in \mathcal{E}$ s.t. (2.3) and (2.5) hold$\}$ consists of flux functions that are, in general, discontinuous across vertices $v \in \mathcal{V}_0 \cup \mathcal{V}_a$, but sum up to zero there. The above function spaces are the natural ones for the problem under consideration. Also note that $u_v \in H^1(0,T)$ is sufficient to obtain a strong solution and that any strong solution (p, m) is (piecewise) Hölder continuous on $[0,T] \times \mathcal{E}$, which follows by embedding. Under stronger regularity assumptions on the data, one can deduce from [27, Theorem 6.1.7] that the strong solution (p, m) is, in fact, classical.

Remark 2.5 (Stability)**.** By the usual energy arguments, one can deduce that the solution of problem (2.1)–(2.9) is also stable under perturbations of the data, i.e., the initial and boundary values $\widehat{p}_0, \widehat{m}_0, \widehat{p}_v, \widehat{m}_v$ and the controls $u = u_v$. In particular, for fixed initial and boundary data, one can estimate the difference $\|p(u) - p(\widetilde{u})\|_{L^\infty(0,T,L^\infty(\mathcal{E}))}$ in the pressure by the difference $\|u - \widetilde{u}\|_{H^1(0,T)}$ of the controls.

The above considerations motivate the following assumption.

Assumption 2.6. The data functions $\widehat{p}_v$, $\widehat{m}_v$, $\widehat{p}_0$, and $\widehat{m}_0$ are chosen such that there exists a control $u \in U_{ad} = \{u \in H^1(0,T) : 0 \le u \le u_{max}\}$, i.e., a Slater point, with the unique strong solution $(p(u), m(u))$ of (2.1)–(2.9) satisfying

$$p_{min} + \eta \le p \le p_{max} - \eta, \qquad \eta > 0.$$

Note that u and $(u, p(u))$ are then, respectively, admissible for the minimization problems (2.16) and (2.14) with $J_R(u) = J(u, p(u)) < \infty$. Moreover, by continuity of the control-to-state map and the continuity of the objective functionals, one obtains that $J_R(\widetilde{u}) = J(\widetilde{u}, p(\widetilde{u})) < \infty$ whenever $\|u - \widetilde{u}\|_{H^1(0,T)}$ is sufficiently small.

The above assumption implies that the system can in fact be controlled in such a way that all consumer demands and constraints can be satisfied simultaneously without violating the technical bounds for the safe operation.

Remark 2.7 (Existence of optimal controls)**.** Existence of optimal controls can now be proven by the usual arguments: By Assumption 2.6, there exist admissible points. We can thus define a minimizing sequences $\{u^n\}$ for $J_R(u)$ which is automatically bounded in $H^1(0,T)$. This allows to extract a sub-sequence that converges weakly in $H^1(0,T)$ to some limit $\bar{u} \in U_{ad}$. Using energy estimates and compact embeddings, the corresponding solutions $p^n = p(u^n)$, $m^n = m(u^n)$ can be shown to strongly converge to $\bar{p} = p(u)$ and $\bar{m} = m(u)$ in L^∞. By convexity of the three terms in the functional $J(u,p)$, one may deduce that $J_R(\bar{u}) = J(\bar{u}, p(\bar{u})) \le \liminf J(u^n, p(u^n)) = \liminf J_R(u^n)$, which establishes the existence of a minimizer.

Under reasonable assumptions on the problem data, the optimal control problem under investigation therefore admits a solution which we now intend to find numerically.

3. Discretization

We now turn to the main scope of the paper, which is the systematic numerical solution of the optimal control problem (2.14). In this section, we discuss the discretization of the state equations and the resulting discrete optimal control problem.

3.1. **Variational characterization of the states.** The following observation will be the starting point for the design of numerical approximation schemes.

Lemma 3.1 (Variational characterization)**.**
Let (p, m) be the strong solution of the problem (2.1)–(2.9) and $\lambda_v = p_v$ for $v \in \mathcal{V}_m$. Then

$$\begin{aligned}
(a\partial_t p(t), q)_{\mathcal{E}} + (\partial_x m(t), q)_{\mathcal{E}} &= 0,\\
(b\partial_t m(t), v)_{\mathcal{E}} - (p(t), \partial_x v)_{\mathcal{E}} &= -(d(p(t), m(t))m(t), v)_{\mathcal{E}} - \langle \widehat{p}_v(t), vn\rangle_{\mathcal{V}_p}\\
&\qquad - \langle \lambda(t), vn\rangle_{V_m} - \langle u(t), v_{out} n_{out}\rangle_{\mathcal{V}_a},\\
\langle m(t), \mu\rangle_{\mathcal{V}_m} &= \langle \widehat{m}(t), \mu\rangle_{\mathcal{V}_m},
\end{aligned}$$

for all $q \in L^2(\mathcal{E})$, $b \in H(div; \mathcal{E})$, and $\lambda \in \mathbb{R}^{|\mathcal{V}_m|}$, and for a.e. $t \in [0, T]$.

Here $(f, g)_{\mathcal{E}} = \sum_{e\in\mathcal{E}} \int_e f_e g_e$ and $\langle f, g\rangle_{\mathcal{V}_i} = \sum_{v\in\mathcal{V}_i} f(v)g(v)$ are used to abbreviate the corresponding scalar products over sets of edges and vertices, respectively.

Proof. The first identity follows by multiplying (2.1) with a test function q_e on every edge $e \in \mathcal{E}$ and summation over all edges. For the second identity, we multiply (2.2) by a test function v_e on every edge and use integration-by-parts. Summing up over all edges and exchanging the order of summation, we then obtain

$$\begin{aligned}
(b\partial_t m(t), v)_{\mathcal{E}} - (p, \partial_x m)_{\mathcal{E}} &= -(d(p, m)m, v)_{\mathcal{E}} - \sum_{e\in\mathcal{E}} \sum_{v\in\mathcal{V}(e)} p_e(v)v_e(v)n_e(v)\\
&= -(d(p, m)m, v)_{\mathcal{E}} - \sum_{v\in\mathcal{V}} \sum_{e\in\mathcal{E}(v)} p_e(v)v_e(v)n_e(v).
\end{aligned}$$

Let us note that $\sum_{e\in\mathcal{E}(v)} v_e(v)n_e(v) = 0$ for all $v \in \mathcal{V}_a \cup \mathcal{V}_0$ since we consider only test-functions $v \in H(\mathrm{div}; \mathcal{E})$. Using the continuity condition (2.4), one can then see that

$$\sum_{v\in\mathcal{V}_0} \sum_{e\in\mathcal{E}(v)} p_e(v)v_e(v)n_e(v) = \sum_{v\in\mathcal{V}_0} p(v) \sum_{e\in\mathcal{E}(v)} v_e(v)n_e(v) = 0,$$

where $p(v) = p_e(v)$, $e \in \mathcal{E}(v)$ is the unique value of the pressure at the vertex v. Next recall that any $v \in \mathcal{V}_a$ is the intersection $v = e_{in} \cap e_{out}$ of exactly two edges and these are ordered according to the orientation of the vertex. In a similar manner as above, we obtain via condition (2.6) that

$$\sum_{v\in\mathcal{V}_a} \sum_{e\in\mathcal{E}(v)} p_e(v)v_e(v)n_e(v) = \sum_{v\in\mathcal{V}_a} u_v v_{e_{out}}(v)n_{e_{out}}(v).$$

Using the boundary conditions (2.8) and $\lambda_v = p_v$ for $v \in \mathcal{V}_m$, we further get

$$\sum_{v\in\mathcal{V}_p\cup\mathcal{V}_m} \sum_{e\in\mathcal{E}(v)} p_e(v)v_e(v)n_e(v) = \sum_{v\in\mathcal{V}_p} \widehat{p}_v v_e(v)n_e(v) + \sum_{v\in\mathcal{V}_m} \lambda_v v_e(v)n_e(v).$$

Here we used that $|\mathcal{E}(v)| = 1$ for boundary vertices $v \in \mathcal{V}_p \cup \mathcal{V}_m$ consequently dropped the summation over edges for these terms. Collecting all intermediate results yields the second identity of the lemma. From (2.7) we directly deduce the third identity. □

3.2. **Discretization in space.** Let $[0, \ell_e]$ be the interval represented by the edge e. We denote by $T_h(e) = \{T\}$ a uniform mesh of e with subintervals T of length h_e. The global mesh is then defined by $T_h(\mathcal{E}) = \{T_h(e) : e \in \mathcal{E}\}$, and the global mesh size is denoted by $h = \max_e h_e$. We denote the spaces of piecewise polynomials on $T_h(\mathcal{E})$ by

$$P_k(T_h(\mathcal{E})) = \{v \in L^2(\mathcal{E}) : v|_e \in P_k(T_h(e)),\ e \in \mathcal{E}\},$$

where $P_k(T_h(e)) = \{v \in L^2(e) : v|_T \in P_k(T),\ T \in T_h(e)\}$ and $P_k(T)$ is the space of polynomials of degree $\leq k$ on the subinterval T. Note that $P_k(T_h(e)) \subset L^2(e)$, which is easy to see, but in general $P_k(T_h(e)) \not\subset H^1(e)$. For the approximation of mass-flux and pressure, we now consider the following finite element spaces

$$V_h = P_1(T_h(\mathcal{E})) \cap H(\mathrm{div}; \mathcal{E}) \quad \text{and} \quad Q_h = P_0(T_h(\mathcal{E})). \tag{3.1}$$

For ease of notation, we further define $\Lambda_h = \mathbb{R}^{|\mathcal{V}_m|}$. By Galerkin approximation of the variational principle of Lemma 3.1, we then obtain the following semi-discrete method.

Problem 3.2 (Semi-discretization)**.**
Find $(p_h, m_h, \lambda_h) \in H^1(0, T; Q_h \times V_h \times \Lambda_h)$ with $p_h(0) = \pi_h \widehat{p}_0$ and $m_h(0) = I_h \widehat{m}_0$ defined as the L^2-projection and piecewise linear interpolation of the initial values, and such that

$$\begin{aligned}
&(a\partial_t p_h(t), q_h)_{\mathcal{E}} + (\partial_x m_h(t), q_h)_{\mathcal{E}} = 0,\\
&(b\partial_t m_h(t), v_h)_{\mathcal{E}} - (p_h(t), \partial_x v_h)_{\mathcal{E}} = -(d(p_h(t), m_h(t))m_h(t), v_h)_{\mathcal{E}} - \langle \widehat{p}_v(t), v_h n\rangle_{\mathcal{V}_p}\\
&\qquad\qquad - \langle \lambda_h(t), v_h n\rangle_{V_m} - \langle u(t), v_{h,out} n_{out}\rangle_{\mathcal{V}_a},\\
&\quad \textit{and} \qquad \langle m_h(t), \mu_h\rangle_{\mathcal{V}_m} = \langle \widehat{m}_h(t), \mu_h\rangle_{\mathcal{V}_m},
\end{aligned}$$

holds for all $q_h \in Q_h$, $v_h \in V_h$, and $\mu_h \in \Lambda_h$, and for a.e. $t \in [0, T]$.

Remark 3.3. In the actual implementation used for our computational tests, we replace the scalar product $(\cdot, \cdot)_{\mathcal{E}}$ in the first and third term of the second equation by

$$(f, g)_{\mathcal{E},h} = \sum_{T \in \mathcal{T}_h(\mathcal{E})} \int_T I_{h,T}(fg)dx,$$

which corresponds to numerical integration via the trapezoidal rule on every mesh element $T \in \mathcal{T}_h(\mathcal{E})$. The use of the approximate scalar product $(\cdot, \cdot)_{\mathcal{E},h}$ for some of the terms facilitates the handling of the nonlinear terms in the discretized state equations and the corresponding discretized optimal control problem but does not play a role in our analysis.

Lemma 3.4. *For any $\widehat{p}_0, \widehat{m}_0 \in L^2(\mathcal{E})$ and $\widehat{p}_v, \widehat{m}_v, \widehat{u}_v \in H^1(0, T)$, Problem 3.2 admits a unique solution (p_h, m_h, λ_h) which continuously depends on the data.*

Proof. By choosing bases for the spaces Q_h, M_h and Λ_h, the semidiscrete variational problem can be turned into an equivalent system of differential algebraic equations

$$\mathbb{M}\partial_t y(t) + \mathbb{A}y(t) + \mathbb{C}y(t) = -\mathbb{D}(y(t))y(t) + \mathbb{B}u(t) + \mathbb{G}(t) \tag{3.2}$$

with $y = (\underline{p}, \underline{m}, \underline{\lambda})$ denoting the coordinate representation of the discrete approximation (p_h, q_h, λ_h) with respect to the chosen basis. The initial values $y(0) = \widehat{y}_0$ can be determined

from the data, the system matrices have the form

$$\mathbb{M} = \begin{pmatrix} M_p & 0 & 0 \\ 0 & M_m & 0 \\ 0 & 0 & 0 \end{pmatrix}, \qquad \mathbb{A} = \begin{pmatrix} 0 & B & 0 \\ -B^\top & 0 & 0 \\ 0 & 0 & 0 \end{pmatrix}, \qquad \mathbb{C} = \begin{pmatrix} 0 & 0 & 0 \\ 0 & 0 & N_m \\ 0 & N_m^\top & 0 \end{pmatrix},$$

$$\mathbb{D}(y) = \begin{pmatrix} 0 & 0 & 0 \\ 0 & D(\underline{p}, \underline{m}) & 0 \\ 0 & 0 & 0 \end{pmatrix}, \qquad \mathbb{B} = \begin{pmatrix} 0 \\ N_a \\ 0 \end{pmatrix},$$

with sub-matrices computed in the usual manner; see e.g. [3]. The data vector $\mathbb{G}(t)$ incorporates the information on the boundary data $\widehat{p}(t)$ and $\widehat{m}(t)$. The Lagrange multiplier $\underline{\lambda}$ can be eliminated from the system using the third equation which leads to a reduced system of ordinary differential equations for $\underline{p}$ and $\underline{m}$; see [8]. Existence of a unique solution then follows from the Picard-Lindelöf theorem, since the nonlinear term $D(\underline{p}, \underline{m})$ is uniformly Lipschitz-continuous, since we assumed $\epsilon > 0$ in the definition of $d(p, m)$. The Lagrange multiplier $\underline{\lambda}$ can be determined uniquely from $(\underline{p}, \underline{m})$ in a post-processing step. □

3.3. **Time discretization.** We choose $N > 0$, set $\tau = T/N$, and define discrete time points $t^n = n\tau$ for $n = 0, \dots, N$. Fllowing the standard convention, we denote by

$$d_\tau f^n = \frac{1}{\tau}(f^n - f^{n-1})$$

the backward difference quotient for a given sequence $\{f^n\}_{n\in\mathbb{N}}$. For the time discretization of Problem 3.2, we then consider the following linear implicit scheme.

Problem 3.5 (Discretized state equation)**.**
Let $\widehat{p}_0, \widehat{m}_0$ and $\widehat{p}_v, \widehat{m}_v$ be the given data. Then set $p_h^0 = \pi_h \widehat{p}_0 \in Q_h$ and $m_h^0 = I_h \widehat{m}(0) \in V_h$ as in Problem 3.2, and for $n = 1, \dots, N$ find $(p_h^n, m_h^n, \lambda_h^n) \in Q_h \times V_h \times \Lambda_h$ such that

$$\begin{aligned} &(a d_\tau p_h^n, q_h)_{\mathcal{E}} + (\partial_x m_h^n, q_h)_{\mathcal{E}} = 0, \\ &(b \partial_t m_h^n, v_h)_{\mathcal{E}} - (p_h^n, \partial_x v_h)_{\mathcal{E}} + (d(p_{min}, m_{max}) m_h^n, v_h)_{\mathcal{E}} + \langle \lambda_h^n, v_h n \rangle_{\mathcal{V}_a} \\ &\qquad\qquad = ([d(p_{min}, m_{max}) - d(p_h^{n-1}, m_h^{n-1})] m_h^{n-1}, v_h)_{\mathcal{E}} \\ &\qquad\qquad\qquad - \langle \widehat{p}_v^n, v_h n \rangle_{\mathcal{V}_p} - \langle \widehat{u}^n, v_{h,out} n_{out} \rangle_{\mathcal{V}_a}, \\ &\quad \textit{and} \qquad \langle m_h^n, \mu_h \rangle_{\mathcal{V}_m} = \langle \widehat{m}^n, \mu_h \rangle_{\mathcal{V}_m}, \end{aligned}$$

for all test functions $q_h \in Q_h$, $v_h \in V_h$, and $\mu_h \in \Lambda_h$. Here and below $\widehat{f}^n = \frac{1}{\tau} \int_{t^{n-1}}^{t^n} f(t) dt$ is used to denote the average of a function f over the time interval $[t^{n-1}, t^n]$.

Remark 3.6. The above scheme amounts to a discontinuous Galerkin approximation of Problem 3.2 in time. The iterates $(p_h^n, m_h^n, \lambda_h^n)$ can therefore be identified with the values of piecewise constant functions $(p_{h,\tau}, m_{h,\tau}, \lambda_{h,\tau})$ of time on the interval $[t^{n-1}, t^n]$. In this spirit, we will call $(p_{h,\tau}, m_{h,\tau})$ the solution of Problem 3.5 in the sequel.

Remark 3.7. To avoid the solution of nonlinear systems in every timestep, we utilize a linear implicit method, which is based on evaluating the damping coefficient $d(p, m)$ at the old time-step. In addition, we added a term of the form $d(p_{min}, m_{max})m$ on both sides

of the second equation. With the notation introduced in the proof of Lemma 3.4, the resulting scheme can be written in algebraic form as

$$[\frac{1}{\tau}\mathbb{M} + \mathbb{A} + \mathbb{C} + \mathbb{D}(\bar{y})]y^n = [\frac{1}{\tau}\mathbb{M} + \mathbb{D}(\bar{y}) - \mathbb{D}(y^{n-1})]y^{n-1} + \mathbb{B}\widehat{u}^n + \widehat{\mathbb{G}}^n, \tag{3.3}$$

with initial value $y^0 = y(0)$ and $\mathbb{D}(\bar{y})$ corresponding to $d(p_{min}, m_{max})$. The system matrices and data vectors defined as in the proof of Lemma 3.4. Note that the matrix on the left hand side is independent of the time-step and therefore has to be factorized only once. The resulting scheme can be seen to be a consistent approximation of first order for the differential-algebraic system (3.2).

From the particular construction of the fully discrete scheme, we deduce the following.

Lemma 3.8. *Problem 3.5 has a unique solution* $(p_h^n, m_h^n, \lambda_h^n)_{n=1,\dots,N} \subset Q_h \times V_h \times \Lambda_h$.

Proof. The system matrix on the left side of equation (3.3) can be shown to be regular; see [8] for details. The assertion then follows by induction. □

Similar as on the continuous and the semidiscrete level, one can again show by means of energy estimates that the discrete solution depends continuously on the data.

3.4. **Discretized optimal control problem.** In order to complete the discretization of the optimal control problem (2.16), let us introduce the space

$$U_\tau = \{u \in H^1(0,T) : u|_{t^{n-1},t^n} \text{ is affine linear}\}$$

of piecewise linear continuous functions of time and denote by

$$U_{ad,\tau} = \{u \in U_\tau : 0 \le u^n \le u_{max},\ 0 \le n \le N\}$$

the set of admissible discretized controls. Note that $U_{ad,\tau} \subset U_{ad}$. As numerical approximation for Problem 2.3, we then consider the following discretized control problem.

Problem 3.9 (Discretized optimal control problem)**.**
For given initial and boundary data $\widehat{p}_0$, $\widehat{m}_0$ *and* $\widehat{p}_v$, $\widehat{m}_v$, *solve*

$$\min_{u_\tau \in U_{ad,\tau}} \|u_\tau\|_{L^1(0,T)} + \frac{\alpha}{2}\|u_\tau\|^2_{H^1(0,T)} + \frac{\beta}{2}\|F(p_{h,\tau}(u_\tau))\|^2_{L^2(\mathcal{E})} \tag{3.4}$$

where $F(p)$ *denotes the barrier function of Problem 2.2 and 2.3 and* $p_{h,\tau}(u_\tau)$ *is the pressure component of the solution of Problem 3.5 with control* $u = u_\tau$.

Remark 3.10. In the statement of the above problem, we again identified the solution of Problem 3.5 with a piecewise constant functions in time.

Since the discretized state equation is uniquely solvable for any choice of $u_\tau \in U_{ad,\tau}$, the discretized control problem always has a minimizer provided the system is controllable at all. It thus makes sense to require the following condition on the problem data.

Assumption 3.11. The initial and boundary data $\widehat{p}_0$, $\widehat{m}_0$ and $\widehat{p}_v$, $\widehat{m}_v$ are chosen such that there exists a discrete optimal control $u_\tau \in U_{ad,\tau}$, a Slater point, with corresponding pressure $p_{h,\tau}(u_\tau)$ defined by Problem 3.5 which satisfies

$$p_{min} + \eta \le p_{h,\tau} \le p_{max} - \eta, \qquad \eta > 0.$$

Note that, as a consequence of this condition and continuity arguments, we have $J_R(\widetilde{u}_\tau) = J(\widetilde{u}_\tau, p_{h,\tau}(\widetilde{u}_\tau)) < \infty$ for all $\widetilde{u} \in U_{ad,\tau}$ with $\|\widetilde{u}_\tau - u_\tau\|$ sufficiently small. Using the continuity of the cost functional and the continuous dependence of the discrete solution $p_{h,\tau}(u_\tau)$ on the discrete control u_τ, we obtain the following result.

Theorem 3.12 (Existence of discrete minimizers)**.**
Let Assumption 3.11 be valid. Then Problem 3.9 has a global minimizer $\bar{u}_\tau \in U_{ad,\tau}$ and any minimizer can be characterized by the variational inequality

$$\langle DJ_R(\bar{u}_\tau), u_\tau - \bar{u}_\tau \rangle \geq 0 \qquad \text{for all } u_\tau \in U_{ad,\tau}, \tag{3.5}$$

where $J_R(u) = J(u, p_{h,\tau}(u))$ is the reduced cost functional, $DJ_R(u)$ denotes its derivative, and $p_{h,\tau}(u)$ is the pressure component of the corresponding solution of Problem 3.5.

Proof. The solution $p_{h,\tau}(u_\tau)$ of Problem 3.5 is continuously differentiable with respect to the control u_τ. Existence of a minimizer for the reduced cost functional then follows from the continuity of J_R and compactness of $U_{ad,\tau}$. The property (3.5) is simply the first order necessary optimality condition for minimizing $J_R(u)$ over $u \in U_{ad,\tau}$. □

4. Practical minimization

After having introduced the discretized optimal control problem, we now turn to the practical minimization procedure. Since the discretized states $(p_{h,\tau}(u_\tau), m_{h,\tau}(u_\tau))$ and also the value of the objective function $J_R(u_\tau) = J(u_\tau, p_{h,\tau}(u_\tau))$ depend smoothly on the control u_τ, we will utilize a Newton-type method of the following form.

Algorithm 4.1 (Projected Netwon-type algorithm)**.**

1: let $u_\tau^{(0)} \in U_{ad,\tau}$ be given and satisfy Assumption 3.11
2: **for** $k = 0, 1, \ldots, K$ **do**
3: choose a convex quadratic approximation $Q^{(k)}(s_\tau)$ of $J_R(u_\tau^{(k)} + s_\tau)$ around $u_\tau^{(k)}$
4: determine $s_\tau^{(k)} \in U_\tau$ by minimizing $Q^{(k)}(s_\tau)$
5: find a stepsize $\omega^{(k)} \in \{1, \frac{1}{2}, \frac{1}{4}, \ldots, \frac{1}{2^N}\}$ such that
6: $\widetilde{u}_\tau^{(k+1)} = \pi_{U_{ad,\tau}}(u_\tau^{(k)} + \omega^{(k)} s_\tau^{(k)})$ and $J_R(\widetilde{u}_\tau^{(k+1)}) < \gamma J_R(u_\tau^{(k)}) - \omega^{(k)} \langle DJ_R(u_\tau^{(k)}), s_\tau^{(k)} \rangle$
7: terminate if no appropriate $\omega^{(k)}$ found or if $\|u_\tau^{(k)} + s_\tau^{(k)} - \pi_{U_{ad,\tau}}(u_\tau^{(k)}) + s_\tau^{(k)}\| < \delta$
8: otherwise, set $u_\tau^{(k+1)} = \widetilde{u}^{(k+1)}$ and continue with loop
9: **end for**

The parameter γ in the Armijo rule has to be chosen between zero and one, and δ will be chosen small to detect when the algorithm starts to stagnate. As a projection to the admissible set, we will utilize in our numerical tests a simple truncation

$$\pi_{U_{ad,\tau}}(u) = \max\{0, \min\{u_{max}, u\}\}.$$

Alternatively, one might also use a projection with respect to the H^1-norm, which requires the solution of a one-dimensional obstacle problem. Together with a specific choice of the quadratic approximations $Q^{(k)}(s_\tau)$, this algorithm will be used for all our numerical examples below. Let us refer to [18] for a convergence analysis and details on the necessary assumptions and minor modifications.

4.1. **Gauss-Newton approximation.** As quadratic approximation $Q^{(k)}(s_\tau)$ of the reduced cost functional $J_R(u_\tau^{(k)+s_\tau})$, we consider in the following the Gauß-Newton approximation

$$Q^{(k)}(s) = (u_\tau^{(k)} + s_\tau, 1)_{L^2(0,T)} + \frac{\alpha}{2}\|u_\tau^{(k)} + s_\tau\|^2_{H^1(0,T)} + \frac{\beta}{2}\|F(p_{h,\tau}) + F'(p_{h,\tau})r_{h,\tau}\|^2_{L^2(0,T;L^2(\mathcal{E}))}, \tag{4.1}$$

where $(p_{h,\tau}, u_{h,\tau})$ is the solution of Problem 3.5 with control $u = u_\tau^{(k)}$, interpreted as a piecewise constant function of time; see Remark 3.6. For the linearization of the first term, we used that $\|u\|_{L^1(0,T)} = \int_0^T u(t)dt$ since $u \geq 0$ for admissible controls. Finally, the function $r_{h,\tau}$ is the pressure component of the solution of the following sensitivity system.

Problem 4.1 (Discrete sensitivity equation)**.**
Let $(p_{h,\tau}, m_{h,\tau})$ denote the solution of Problem 3.5 for control $u \in U_{ad,\tau}$ and $s_\tau \in U_\tau$ be given. Set $r_h^0 = 0, w_h^0 = 0$, and for $1 \leq n \leq N$, find $(r_h^n, w_h^n, \xi_h^n) \in Q_h \times V_h \times \Lambda_h$, such that

$$\begin{aligned}
&(ad_\tau r_h^n, q_h)_{\mathcal{E}} + (\partial_x w_h^n, q_h)_{\mathcal{E}} = 0,\\
&(b\partial_t w_h^n, v_h)_{\mathcal{E}} - (r_h^n, \partial_x v_h)_{\mathcal{E}} + (d(p_{min}, m_{max})w_h^n, v_h)_{\mathcal{E}} + \langle \xi_h^n, v_h n\rangle_{\mathcal{V}_a}\\
&\qquad = ([d(p_{min}, m_{max}) - d(p_h^{n-1}, m_h^{n-1}) - d'_m(p_h^{n-1}, m_h^{n-1})m_h^{n-1}]w_h^{n-1}, v_h)_{\mathcal{E}}\\
&\qquad\qquad - (d'_p(p_h^{n-1}, m_h^{n-1})m_h^{n-1}r_h^{n-1}, v_h)_{\mathcal{E}} - \langle \widehat{s}^n, v_{h,out}n_{out}\rangle_{\mathcal{V}_a},\\
&\textit{and} \qquad \langle w_h^n, \mu_h\rangle_{\mathcal{V}_m} = 0,
\end{aligned}$$

for all test functions $q_h \in Q_h$, $v_h \in V_h$, and $\mu_h \in \Lambda_h$.

Let us recall that $\widehat{s}^n = \frac{1}{\tau}\int_{t^{n-1}}^{t^n} s(t)dt$ denotes the local average of the function s. Moreover, we will again denote by $(r_{h,\tau}, w_{h,\tau})$ the corresponding piecewise constant functions with values (r_h^n, w_h^n) on the respective time interval.

Remark 4.2. With the notation used in the proof of Lemma 3.4 and in Remark 3.7, the sensitivity problem can be written in algebraic form as

$$[\frac{1}{\tau}\mathbb{M} + \mathbb{A} + \mathbb{C} + \mathbb{D}(\bar{y})]z^n = [\frac{1}{\tau}\mathbb{M} + \mathbb{D}(\bar{y}) - \mathbb{D}(y^{n-1}) - \mathbb{D}'(y^{n-1})y^{n-1}]z^{n-1} + \mathbb{B}\widehat{s}^n,$$

with initial value $z^0 = 0$. Here $D(y^{n-1}) + D'(y^{n-1})y^{n-1}$ denotes the matrix stemming from differentiation of the vector $D(y^{n-1})y^{n-1}$. Existence of a unique solution again follows directly from the regularity of the system matrix on the left hand side.

The following result follows immediately from the construction of the sensitivity problem.

Lemma 4.3 (Sensitivity system)**.**
For any $u_\tau \in U_{ad,\tau}$ and $s_\tau \in U_\tau$, Problem 4.1 has a unique solution $(r_{h,\tau}, w_{h,\tau})$. Moreover,

$$r_{h,\tau} = \lim_{\epsilon\to 0}\frac{1}{\epsilon}(p_{h,\tau}(u_\tau + \epsilon s_\tau) - p_{h,\tau}(u_\tau)) \quad \textit{and} \quad w_{h,\tau} = \lim_{\epsilon\to 0}\frac{1}{\epsilon}(m_{h,\tau}(u_\tau + \epsilon s_\tau) - m_{h,\tau}(u_\tau)),$$

i.e., $(r_{h,\tau}, w_{h,\tau})$ is the derivative of $(p_{h,\tau}(u_\tau), m_{h,\tau}(u_\tau))$ with respect to u_τ in direction s_τ.

4.2. **Minimization of the quadratic approximation.** The quadratic Gauß-Newton approximation of the reduced cost functional $J_R(u_\tau^{(k)} + s_\tau)$ can formally be written in the form

$$Q^{(k)}(s_\tau) = Q_0^{(k)} + \langle DQ^{(k)}, s_\tau\rangle + \frac{1}{2}\langle HQ^{(k)}s_\tau, s_\tau\rangle.$$

Here $\langle\cdot,\cdot\rangle$ is a duality product which, on the algebraic level, can be chosen as the Euclidean scalar product. The minimizer of $Q^{(k)}(s_\tau)$ can thus be computed by solving

$$\langle HQ^{(k)}s_\tau, \sigma_\tau\rangle = -\langle DQ^{(k)}, \sigma_\tau\rangle \qquad \text{for all } \sigma_\tau \in U_\tau. \tag{4.2}$$

We use a variational formulation of the optimality condition here to underline the functional analytic background and to simplify the notation in our following considerations.

Remark 4.4. On the algebraic level, equation (4.2) amounts to the linear system

$$HQ^{(k)}s = -DQ^{(k)}, \tag{4.3}$$

where s is the coordinate representation of the control s_τ and where we tacitly identified the linear functional $DQ^{(k)}$ and the linear operator $HQ^{(k)}$ with their respective matrix representations. Let us note that $HQ^{(k)}$ will be a symmetric and positive definite matrix, if an appropriate discrete duality product is chosen for its definition on the algebraic level. The system (4.3) can therefore be solved efficiently by a (preconditioned) conjugate gradient method which only requires assembly of the Jacobian vector $DQ^{(k)}$ and access to the matrix-vector product $HQ^{(k)}\cdot s$ of the control vector s with the Hessian matrix.

4.3. **Representation of the Jacobian and Hessian via adjoints.** Before completing our considerations about the numerical solution of the discretized optimal control problem, let us briefly discuss the efficient realization of the Jacobian $DQ^{(k)}$ and of the Hessian $HQ^{(k)}$ via solutions of adjoint problems. We start with deriving a convenient representation for the Jacobian. A formal differentiation of the functional (4.1) yields

$$\begin{aligned}\langle DQ^{(k)}, s_\tau\rangle = (1, s_\tau)_{L^2(0,T)} &+ \alpha(u_\tau^{(k)}, s_\tau)_{H^1(0,T)} \\ &+ \beta(F(p_{h,\tau}), F'(p_{h,\tau})r_{h,\tau})_{L^2(0,T;L^2(\mathcal{E}))},\end{aligned}$$

where $(p_{h,\tau}, m_{h,\tau})$ is the solution of Problem 3.5 for control $u = u_\tau^{(k)}$, and $r_{h,\tau}$ is the pressure component of the derivative of $(p_{h,\tau}(u_\tau), m_{h,\tau}(u_\tau))$ with respect to u_τ in direction s_τ, as defined in Problem 4.1. For computing the last term in an efficient way, we make use of the solutions to the following adjoint problem.

Problem 4.5 (Discretized adjoint equation)**.**
Let $(p_{h,\tau}, m_{h,\tau})$ denote the solution of Problem 3.5 for control $u \in U_{ad,\tau}$ and let $f_{h,\tau}$ be a given piecewise constant function of time with values in $f_h^n \in Q_h$. Then set $\widetilde{r}_h^{N+1} = 0$ and $\widetilde{w}_h^{N+1} = 0$, and for $N \geq n \geq 1$, find $(\widetilde{r}_h^n, \widetilde{w}_h^n, \widetilde{\xi}_h^n) \in Q_h \times V_h \times \Lambda_h$, such that

$$\begin{aligned}(ad_\tau\widetilde{r}_h^{n+1}, q_h)_\mathcal{E} + (\partial_x\widetilde{w}_h^n, q_h)_\mathcal{E} &= (d_p'(p_h^n, m_h^n)m_h^n\widetilde{m}_h^{n+1}, q_h)_\mathcal{E} + (f_h^n, q_h)_\mathcal{E},\\ (b\partial_t\widetilde{w}_h^n, v_h)_\mathcal{E} - (\widetilde{r}_h^n, \partial_x v_h)_\mathcal{E} - (d(p_{min}, m_{max})\widetilde{w}_h^n, v_h)_\mathcal{E} &+ \langle\widetilde{\xi}_h^n, v_h n\rangle_{\mathcal{V}_a}\\ &= ([d(p_h^n, m_h^n) - d(p_{min}, m_{max}) + d_m'(p_h^n, m_h^n)m_h^n]\widetilde{w}_h^{n+1}, v_h)_\mathcal{E}\\ \text{and}\qquad \langle\widetilde{w}_h^n, \mu_h\rangle_{\mathcal{V}_m} &= 0,\end{aligned}$$

for all $q_h \in Q_h$, $v_h \in V_h$, and $\mu_h \in \Lambda_h$. We again denote by $(\widetilde{r}_{h,\tau}, \widetilde{w}_{h,\tau})$ the corresponding piecewise constant functions of time with values $(\widetilde{r}_h^n, \widetilde{w}_h^n)$ on the respective time intervals.

Remark 4.6. With the notation used in the proof of Lemma 3.4 and in Remark 3.7, the algebraic representation of the adjoint problem is given by

$$[\frac{1}{\tau}\mathbb{M} + \mathbb{A}^\top + \mathbb{C} + \mathbb{D}(\bar{y})]\widetilde{z}^n = [\frac{1}{\tau}\mathbb{M} + \mathbb{D}(\bar{y}) - \mathbb{D}(y^n) - \mathbb{D}'(y^n)^\top y^n]\widetilde{z}^{n+1} + \mathbb{F}^n,$$

for $n = N, \dots, 1$ with terminal value $\widetilde{z}^{N+1} = 0$ and $\mathbb{F}^n$ representing the term with f_h^n. Using the arguments of [8], the system matrix on the left hand side can again be seen to be regular, which yields the well-posedness of the discretized adjoint problem.

With the help of the adjoint solution $(\widetilde{r}_{h,\tau}, \widetilde{w}_{h,\tau})$ defined by Problem 4.5, we can now represent the Jacobian $DQ^{(k)}$ in the following convenient way.

Lemma 4.7 (Representation of the Jacobian)**.**
Let $(p_{h,\tau}, m_{h,\tau})$ be the solution of Problem 3.5 for control $u = u_\tau \in U_{ad,\tau}$ and let $(\widetilde{r}_{h,\tau}, \widetilde{w}_{h,\tau})$ be the corresponding adjoint solution of Problem 4.5 with data $f_{h,\tau} = F'(p_{h,\tau})F(p_{h,\tau})$. Then

$$\langle DQ^{(k)}, s_\tau \rangle = (d_\tau, s_\tau)_{H^1(0,T)}$$

where $d_\tau \in U_\tau$ is the unique weak solution of

$$(d_\tau, s_\tau)_{H^1(0,T)} = (1, s_\tau)_{L^2(0,T)} + \alpha(e_\tau, s_\tau)_{H^1(0,T)} + \beta(\widetilde{w}_{h,\tau;out} n_{out}, s_\tau)_{L^2(0,T)}.$$

Proof. The first two terms in the representation are obtained directly from the definition of $DQ^{(k)}$. For the third term, let us observe that by definition of $(\widetilde{r}_{h,\tau}, \widetilde{w}_{h,\tau})$, we have

$$\begin{aligned}(F(p_{h,\tau}),F'(p_{h,\tau})r_{h,\tau})_{L^2(0,T;L^2(\mathcal{E})} &= \sum_{n=1}^{N} \tau(F'(p_h^n)F(p_h^n), r_h^n) \\ &= \sum_{n=1}^{N} \tau(ad_\tau \widetilde{p}_h^{n+1}, r_h^n)_{\mathcal{E}} + (\partial_x \widetilde{w}_h^n, r_h^n)_{\mathcal{E}}.\end{aligned}$$

Employing the discrete variational characterizations of $(r_{h,\tau}, w_{h,\tau})$ and $(\widetilde{r}_{h,\tau}, \widetilde{w}_{h,\tau})$ given in Problem 4.1 and 4.5, one can see, after a sequence of elementary manipulations, that

$$\sum_{n=1}^{N} \tau(ad_\tau \widetilde{p}_h^{n+1}, r_h^n)_{\mathcal{E}} + (\partial_x \widetilde{w}_h^n, r_h^n)_{\mathcal{E}} = \sum_{n=1}^{N} \tau \langle \widehat{s}^n, \widetilde{w}_{h,out}^n n_{out} \rangle_{\mathcal{V}_a}.$$

The last term corresponds to the third term in the above representation of the Jacobian, which already completes the proof of the assertion. □

Remark 4.8 (Computation of the Jacobian)**.**
Let M and K denote the finite element matrices representing the scalar products $(u, v)_{L^2(0,T)}$ and $(u, v)_{H^1(0,T)}$. Then the Jacobian $d = DQ^{(k)}$ is characterized in algebraic form as

$$Md = M1 + \alpha Ku + G,$$

where 1 is the constant one vector and G can be computed from the values $w_{h,out}^n$ of the adjoint flux function at the vertex $v \in \mathcal{V}_a$. The Jacobian $DQ^{(k)}$ can thus be computed efficiently by solving one adjoint problem and some elementary computations.

As a last step in our theoretical considerations, we now also derive an efficient representation for the multiplication $HQ^{(k)}s_\tau$ of a discretized control s_τ with the Hessian.

Lemma 4.9 (Representation of the Hessian)**.**
Let $(p_{h,\tau}, m_{h,\tau})$ be the solution of Problem 3.5 for control $u \in U_{ad,\tau}$, and let $(w_{h,\tau}, r_{h,\tau})$ denote the corresponding sensitivity defined by Problem 4.1 with direction s_τ. Then

$$\langle HQ^{(k)} s_\tau, \sigma_\tau \rangle = (h_\tau, \sigma_\tau)_{H^1(0,T)}$$

where $h_\tau \in U_\tau$ is the unique weak solution of

$$(h_\tau, \sigma_\tau)_{H^1(0,T)} = \alpha (s_\tau, \sigma_\tau)_{H^1(0,T)} + \beta (\widetilde{w}_{h,\tau;out} n_{out}, \sigma_\tau)_{L^2(0,T)},$$

and where $(\widetilde{r}_{h,\tau}, \widetilde{w}_{h,\tau})$ is the solution of Problem 4.5 with input data $f_{h,\tau} = |F'(p_{h,\tau})|^2 r_{h,\tau}$.

Proof. The assertion is obtained in a similar manner as that of the previous lemma. □

5. Numerical results

To validate our theoretical results and to demonstrate the performance of the proposed algorithms, we now present some computational results for two test problems that model typical scenarios in the daily operation of a gas network. In both test problems, the network consists of a few pipes, each of which is partitioned into the same number ne of elements $T \in T_h(e)$. The time interval $[0, T]$ is divided into nt time segments of uniform length $\tau = T/nt$. The properties of the gas are encoded in the speed of sound, which is chosen to be a constant $c = 376$ [m/s] for all our tests. The properties of the individual pipes, i.e., the length ℓ_e, the diameter D_e, the cross-section A_e, and the friction factor λ_e will be specified below. The lumped parameters a_e, b_e, and d_e arising in the equations (2.1)–(2.2) are defined as $a_e = A_e/c^2$, $b_e = 1/A_e$, and

$$d_e(p_e, m_e) = \max\{\epsilon, \min\{1/\epsilon, \frac{\lambda_e}{2D_e} \frac{c^2}{A_e^2} \frac{|m_e|}{p_e}\}\}.$$

In our numerical tests, the truncation parameter is set to $\epsilon = 10^{-3}$ and, due to the state constraints in the optimization problem, the truncation in fact never becomes active.

5.1. **Two pipes, one compressor.** As a first test scenario, we consider the transport through a long pipe $e_1 \cup e_2$ which is mainteind by a compressor located at vertex v_C in the middle of the two pipe segments; see Figure 5.1.

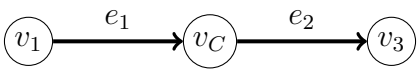

Figure 5.1. Topology of the two pipe system.

The specifications of the two pipes are chosen as

$$\ell_e = 10 \text{ [km]}, \quad D_e = 1 \text{ [m]}, \quad A_e = 0.785 \text{ [m}^2\text{]}, \quad \text{and} \quad \lambda_e = 0.01 \text{ []}.$$

The technical bounds for pipes and compressor are given by

$$p_{min} = 77 \text{ [bar]}, \quad p_{max} = 81 \text{ [bar]}, \quad m_{max} = 500 \text{ [kg/s]}, \quad \text{and} \quad u_{max} = 4 \text{ [bar]}.$$

We assume that gas is supplied at constant pressure at the left entry of the pipe system, and that the demand of gas is continuously increasing at the right end of the network. This is modeled by the boundary conditions

$$\widehat{p}_{v_1}(t) = 80 \text{ [bar]} \quad \text{and} \quad \widehat{m}_{v_3}(t) = 20 \cdot t \text{ [kg/s]}.$$

The initial conditions are chosen as stationary solutions which are compatible with these boundary conditions at time $t = 0$. For the choice taken above, this yields

$$\widehat{p}_0 \equiv 80 \text{ [bar]} \quad \text{and} \quad \widehat{m}_0 \equiv 0 \text{ [kg/s]}.$$

We then solve the optimal control problem (2.14) with regularization parameter $\alpha = 10^{-1}$, barrier parameter $\beta = 10^{-8}$, and discretization parameters $n_e = n_t = 400$.

Numerical results. For our numerical tests, we consider a time horizon of $T = 20$ [h]. As initial guess for the Gauß-Newton iteration, we choose

$$u_\tau^{(0)} = 0.1 \cdot t \text{ [bar]}.$$

Th corresponding pressure $p_{h,\tau}(u_\tau^{(0)})$ defined by Problem 3.5 then satisfies the given state constraints, i.e., Assumption 3.11 is valid.

In Figure 5.2, we display the iterates $u_\tau^{(k)}$, $k = 0, \ldots, 5$ computed by the Gauß-Newton iteration and we also plot the corresponding pressure profiles $p(\cdot, t)$ for some points in time. In our computational test, the Gauß-Newton iteration terminated after 5 iterations, since

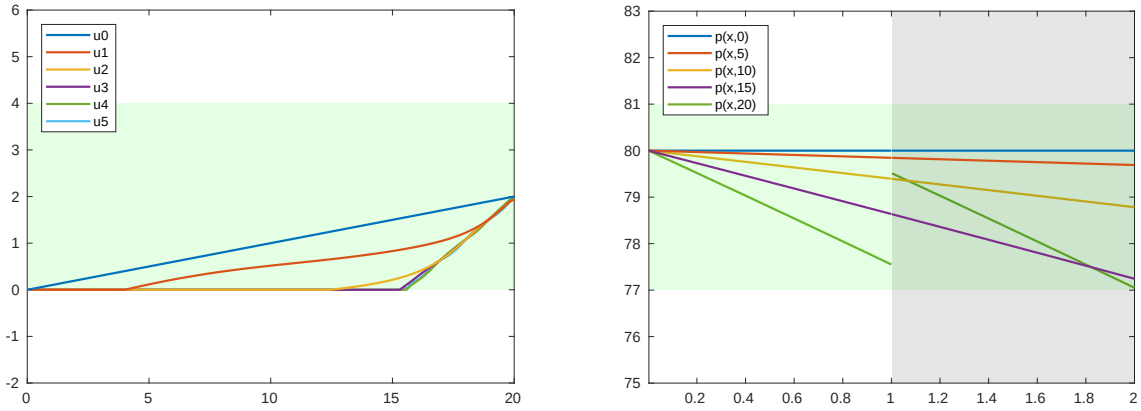

FIGURE 5.2. Left: Control iterates $u_\tau^{(k)}$ generated by the Gauß-Newton method outlined in Section 4. Right: Pressure profile $p_{h,\tau}(u_\tau^{(5)})$ for different times $t \in [0, 5, 10, 15, 20]$ obtained by solution of Problem 3.5. The grean areas denote the admissible regions. The white and gray background in the right plot marks the two different pipes.

the update became too small. A total number of 81 cg-iterations was required for the solution of the linearized problems. The computed optimal control here stays zero as long as the demands can be satisfied by the pressure drop in the pipe. Around $t = 15$, the compressor starts to work and compressor power is gradually increased to compensate for the increasing demand at the right end and to avoid violation of the lower bound for the pressure at the outflow vertex v_3. As expected, the L^1-term in the cost functional promotes a sparse solution, i.e., the optimal control is set to zero where possible. The regularizing H^1-term in the cost functional, on the oterh hand, leads to a piecewise smooth optimal control. The barrier term in the objective functional finally guarantees the validity of the state constraints on the period of time.

Mesh independence. To illustrate the mesh independence of our approach, we run the above computations with the same model parameters but for a sequence of different discretization parameters. The corresponding results are summarized in Table 5.1.

$n_t = n_e$	$J_R(\bar{u})$	#Newton	#cg-iter.
25	4.80	6	46
50	4.78	3	30
100	4.79	4	54
200	4.79	4	60
400	4.77	5	81

TABLE 5.1. Optimal function values and iteration numbers for Gauß-Newton method depending on the discretization parameters.

Due to the underlying functional analytic setting, the number of iterations required for the minimization process is almost independent of the mesh size. Let us mention that also the corresponding optimal controls obtained for different discretization parameters are almost indistinguishable.

5.2. **Five pipes, one compressor, one regulator.** With the second test case, we would like to demonstrate the applicability of our algorithms for more general situations, e.g., to problems involving multiple active elements or additial constraints, cf. Remark 2.1. As network topology, we here consider the network depicted in Figure 5.3 that was already used in Section 2 to illustrate our notation.

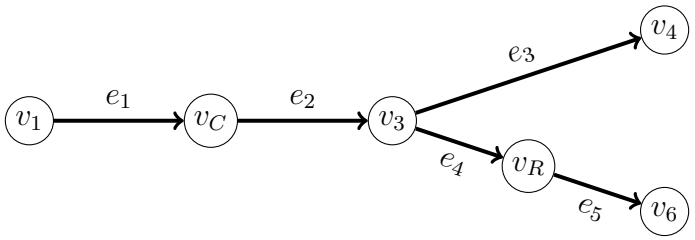

FIGURE 5.3. Network consisting of five pipes and two active elements, i.e., one commpressor and one regulator located at vertex v_C and v_R.

Similar as in the previous example, gas is supplied at constant pressure at the entry v_1, and two customers, a gas-fueled power plant and a local gas supplier, take out gas the the exits v_4 and v_6. A compressor located at vertex v_C can be controlled in order to provide the requested mass flux and a regulatro at vertex v_R can reduce the pressure for the pipe e_5. The specifications of the pipes are chosen as in the previous example. In addition, we assume that the pressure and mass flux are constrained from above and below by

$$p_{min,e} \le p_e \le p_{max_e} \quad \text{and} \qquad ,_{min,e} \le m_e \le m_{max,e}$$

with technical bounds specified for the support pipes e_1, e_2, e_3, e_4 as

$$p_{min,e} = 55 \text{ [bar]}, \quad p_{max,e} = 80 \text{ [bar]}, \quad m_{min,e} = -20 \text{ [kg/s]}, \quad m_{max,e} = 700 \text{ [kg/s]}$$

For the last pipe e_5, we require different pressure bounds

$$p_{min,e_5} = 42 \text{ [bar]}, \quad p_{max,e_5} = 63,$$

while the bounds for the mass flux are chosen the same as for the other pipes. As constraints for the two controls u_C and u_R, which limit the minimal and maximal amount of increase or reduction of the pressure across the respective element, we choose

$$0 \leq u_C \leq u_{C,max} = 15 \text{ [bar]} \qquad \text{and} \qquad 0 \leq u_R \leq u_{R,max} = 15\text{[bar]}.$$

Similar as in the previous example, the time varying customer demands are modeled by the boundary conditions. Here we choose

$$\widehat{p}_{v_1}(t) = 70 \text{ [bar]}, \qquad \widehat{m}_{v_6}(t) = 200 \text{ [kg/s]},$$
$$\widehat{m}_{v_4}(t) = \max(0, \min(400, 400 \cdot (t - 10))) \text{ [kg/s]},$$

which models a situation, where the power plant located at vertex v_C starts to operate around time $t = 10$ [h], which leads to a drastic increase in demand, while the local gas supplier at v_6 extracts gas at a constant rate. As initial data, we here choose the stationary solution obtained with the boundary conditions $p_{v_1} = 70$ [bar], $m_{v_4} = 0$ [kg/s], and $m_{v_6} = 200$ [bar] and for fixed controls $u_C = 5$ and $u_R = 15$. This choice is compatible with the data for the instationary problem.

Numerical results. For our computations, we again consider a time horizon of $T = 20$ [h]. As initial guess for the control required in the Gauß-Newton iteration, we choose

$$u^{(0)} = (u_C^{(0)}(t), u_R^{(0)}(t)) = (5 + 0.5 \cdot t, 15) \text{ [bar]}.$$

These values are chosen such that the corresponding solution $(p_{h,\tau}(u^{(0)}), m_{h,\tau}(u_\tau^{(0)}))$ of Problem 3.5 satisfies the given state constraints.

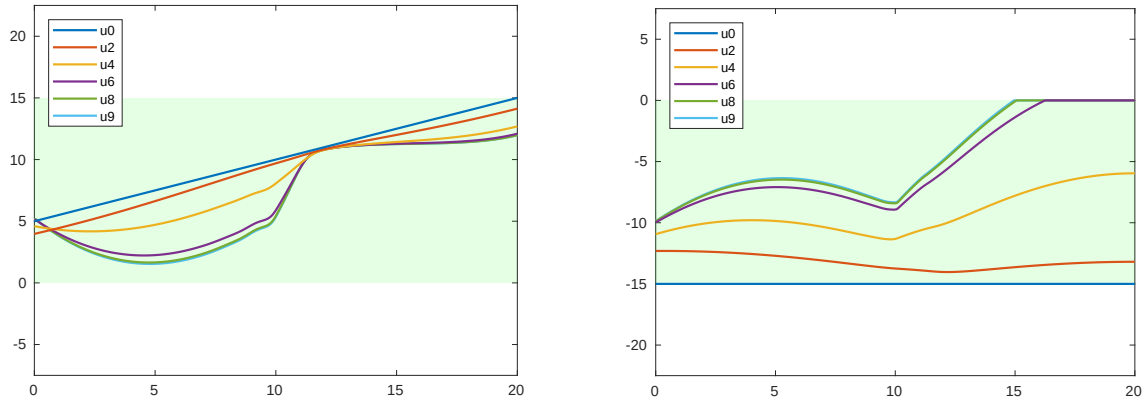

FIGURE 5.4. Control iterates $u_{C,\tau}^{(k)}$ (left) for the compressor at vertex v_2 and $-u_{R,\tau}^{(k)}$ (right) for the regulator at vertex v_5 obtained with the projected Gauß-Newton method outlined in Section 4.

In Figure 5.4 and 5.5, we display the control iterates $u_\tau^{(k)}$ for compressor and regulator and some snapshots for the corresponding pressures and mass fluxes obtained in our simulations. For our computations, we chose the discretization parameters $n_t = n_e = 400$, the regularization parameter $\alpha = 10^{-1}$, and the barrier parameter $\beta = 10^{-5}$. The solution

of the optimal control problem required 11 Newton-iterations and in total 241 cg-iterations for the solution of the linear system in the Gauß-Newton iteration.

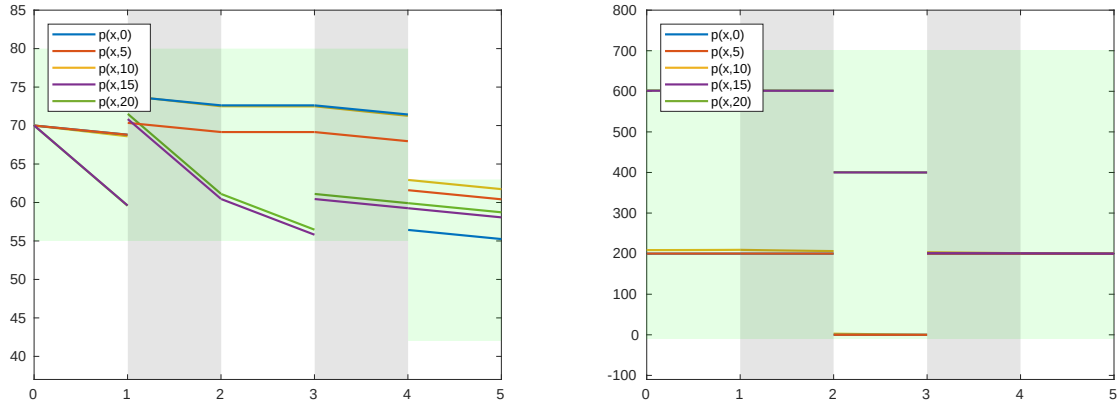

FIGURE 5.5. Snapshots of the pressure $p_{h,\tau}(\bar{u}_\tau)$ (left) and mass flux $m_{h,\tau}(\bar{u}_\tau)$ (right) for different times $t = 0, \ldots, 20$ obtained with the optimal control $\bar{u}_\tau$ displayed in Figure 5.4.

Let us briefly discuss the results in the context of the specific application. First, we can observe that the compressor power is reduced in the beginning, since the pressure difference between the vertex v_1 and the vertex v_6 alone already suffices to transport the gas to the local gas supplier at vertex v_6. This leads to a slight backflow of gas from the pipe e_3 into the vertex v_3; see Figure 5.5. The lower bounds on the mass flux enforce that the compressor, and also the regulator, can be turned down only gradually. At time $t = 10$, the power plant suddenly increases the gas demand at the vertex v_4. This is compensated by turning up the compressor again. The large flux through pipe e_3 however still leads to a decrease in pressure at the vertex v_3 and also in the pipe e_4. Therefore, the regulator at the vertex v_R can be switched off completely. Some more complicated transition takes place in an interval around time $t = 10$ which we cannot fully explain by such simple arguments. Overall, the optimal controls however seem reasonable from a practical point of view.

6. SUMMARY

In this paper, we considered the systematic numerical solution of optimal control problems arising in the daily operation of gas networks. A semilinear hyperbolic system of partial differential-algebraic equations was used as a model for the gas flow on the network. We discussed the well-posedness of this system and the resulting optimal control problems. For the numerical solution, we considered a Galerkin approximation by mixed finite elements and proposed a linear implicit time integration scheme which can be interpreted as a discontinuous Galerkin approximation. The proposed discretization of the state equations was considered in function spaces which allowed us to establish well-posedness of the discretized state equations and the existence of minimizers for the discretized optimal control problem. For the numerical solution of the optimization problem, we considered a projected Gauß-Newton method. For minimizing the quadratic approximations for the nonlinear cost functional, we employed a conjugate gradient method and we discussed

the efficient assembly of the Jacobian and the application of the Hessian via the solution of sensitivity and ajoint problems. Due to the variational foundation of the discretization scheme, the discrete adjoint problems automatically leas to a valid discretization of the continuous adjoint equations. Our methods therefore do not suffer from problems with first-discretize-then-optimize approaches. The viability of the proposed methods and their performance were illustrated with numerical tests that were designed to reflect typical scenarios that might arise during operation of a gas network.

While in our preliminary computational tests, the proposed methods worke very well, there are also some issues that should be addressed in future research: In our approach, we incorporated the state constraints via a barrier function with a fixed barrier parameter β. While this might be sufficient for practical purposes, where one would probably not like to operate the network too close to the technical bounds, it would be interesting to study path following methods to find the optimal β. Also the use of other regularization terms, e.g., the $W^{1,1}$-norm, might be interesting to be studied in future. Finally, the consideration of appropriate globalization strategies in the projected Gauß-Newton method may be of significant relevance for practical applications.

Acknowledgments

The authors are grateful for financial support by the German Research Foundation (DAG) via grants IRTG 1529 and TRR 154 projects A08 and C04, and by the "Excellence Initiative" of the German Federal and State Governments via the Graduate School of Computational Engineering GSC 233 at Technische Universität Darmstadt.

References

[1] A. Bamberger, M. Sorine, and J. P. Yvon. Analyse et contrôl d'un réseau de transport de gaz. volume 91 of *Lecture Notes in Physics*, pages 345–359.
[2] C. Berge. *Graphs. 2nd rev.* North-Holland, Amsterdam, New York, Oxford, 1985.
[3] D. Braess. *Finite Elements.* Cambridge University Press, New York, 3rd edition, 2007.
[4] J. Brouwer, I. Gasser, and M. Herty. Gas pipeline models revisited: Model hierarchies, non-isothermal models and simulations of networks. *Multiscale Model. Simul.*, 9:601–623, 2011.
[5] J. Brouwer, I. Gasser, and M. Herty. Gas pipeline models revisited: Model hierarchies, nonisothermal models, and simulations of networks. *Multiscale Modeling and Simulation*, 9:601–623, 2011.
[6] P. Domschke, B. Geißler, O. Kolb, J. Lang, A. Martin, and A. Morsi. Combination of nonlinear and linear optimization of transient gas networks. *INFORMS J. Comput.*, 23:605–617, 2011.
[7] P. Domschke, O. Kolb, and J. Lang. Adjoint-based error control for the simulation and optimization of fas and water supply networks. *Appl. Num. Math.*, 259:1003–1018, 2015.
[8] H. Egger, T. Kugler, B. Liljegren-Sailer, N. Marheineke, and V. Mehrmann. On structure-preserving model reduction for damped wave propagation in transport networks. Technical report, TRR 154, 2017. arXive:1704.03206.
[9] L. C. Evans. *Partial Differential Equations.* American Mathematical Society, 1998.
[10] B. P. Furey. A sequential quadratic programming-based algorithm for optimization of gas networks. *Automatica*, 29:1439–1450, 1993.
[11] S. Göttlich, M. Herty, and A. Klar. Network models for supply chains. *Commun. Math. Sci.*, 3:545–559, 2005.
[12] M. Gugat, M. Dick, and G. Leugering. Gas flow in fan-shaped networks: classical solutions and feedback stabilization. *SIAM J. Control Optim.*, 49:2101–2117, 2011.
[13] M. Gugat, M. Herty, A. Klar, and G. Leugering. Optimal control of traffic flow networks. *J. Optim. Theory Appl.*, 236:589–616, 2005.
[14] M. Gugat, M. Herty, and V. Schleper. Flow control in gas networks: Exact controllability to a given demand. *Math. Meth. Appl. Sci.*, 34:745–757, 2011.

[15] W. W. Hager. Runge-Kutta methods in optimal control and the transformed adjoint system. *Numer. Math.*, 87(2):247–282, 2000.
[16] M. Hahn, S. Leyffer, and V. M. Zavala. Mixed-integer PDE-constrained optimal control of gas networks. Technical Report MCS-P7095-0917, August 2017.
[17] M. Herty, A. Kurganov, and D. Kurochkin. Numerical method for optimal control problems governed by nonlinear hyperbolic systems of PDEs. *Commun. Math. Sci.*, 13:15–48, 2015.
[18] M. Hinze, R. Pinnau, M. Ulbrich, and S. Ulbrich. *Optimization with PDE constraints*, volume 23 of *Mathematical Modelling: Theory and Applications*. Springer, New York, 2009.
[19] C. Kirchner, M. Herty, S. Göttlich, and A. Klar. Optimal control for continuous supply network models. *Netw. Heterog. Media*, 1:675–688, 2006.
[20] T. Koch, B. Hiller, M. E. Pfetsch, and L. Schewe, editors. *Evaluating Gas Network Capacities*. SIAM-MOS series on Optimization. SIAM, 2015.
[21] F. Kruse and M. Ulbrich. A self-concordant interior point approach for optimal control with state constraints. *SIAM J. Optim.*, 25(2):770–806, 2015.
[22] J. L. Lions. *Optimal Control of Systems Governed by Partial Differential Equations*. Springer-Verlag, Berlin, 1971.
[23] D. Mahlke, A. Martin, and S. Moritz. A simulated annealing algorithm for transient optimization in gas networks. *Math. Meth. Oper. Res.*, 66:99–115, 2007.
[24] A. Martin, M. Möller, and S. Moritz. Mixed Integer Models for the Stationary Case of Gas Network Optimization. *Mathematical Programming, Series B*, 105:563–582, 2006.
[25] D. Mugnolo. *Semigroup methods for evolution equations on networks*. Springer, Cham, 2014.
[26] A. J. Osiadacz. Different transient models – limitations, advantages and disadvantages. Technical report, PSIG report 9606, Pipeline Simulation Interest Group, 1996.
[27] A. Pazy. *Semigroups of Linear Operators and Applications to Partial Differential Equations*. Springer-Verlag, New York, 1983.
[28] E. Polak. *Optimization: Algorithms and consistent approximations*, volume 124 of *Applied Mathematical Sciences*. Springer-Verlag, 1997.
[29] R. Z. Ríos-Mercado and C. Borraz-Sánchez. Optimization problems in natural gas transportation systems: A state-of-the-art review. *Applied Energy*, 147:536–555, 2015.
[30] A. Schiela. Barrier methods for optimal control problems with state constraints. *SIAM J. Optim.*, 20(2):1002–1031, 2009.
[31] A. Schiela and W. Wollner. Barrier methods for optimal control problems with convex nonlinear gradient state constraints. *SIAM J. Optim.*, 21(1):269–286, 2011.
[32] M. A. Stoner. Analysis and control of unsteady flows in natural gas piping systems. *Trans. ASME*, pages 331–340, 1969.
[33] F. Tröltzsch. *Optimal Control of Partial Differential Equations: Theory, Methods and Applications*. Graduate Studies in Mathematics. AMS, 2010.
[34] S. Ulbrich. *Optimal Control of Nonlinear Hyperbolic Conservation Laws with Source Terms*. Habilitation thesis, Technische Universität München, 2001.
[35] P. J. Wong and R. E. Larson. Optimization of natural-gas pipeline systems via dynamic programming. *IEEE Trans. Aut. Cont.*, AC-13:475–481, 1968.
[36] P. J. Wong and R. E. Larson. Optimization of tree-structured natural-gas transmission networks. *J. Math. Anal. Appl.*, 24:613–626, 1968.